Spinal Cord (2011) 49, 345–351
© 2011 International Spinal Cord Society All rights reserved 1362-4393/11 $32.00
www.nature.com/sc

ORIGINAL ARTICLE

Post-mortem assessment of rat spinal cord injury and white matter sparing using inversion recovery-supported proton density magnetic resonance imaging

F Scholtes[1,2], E Theunissen[3], R Phan-Ba[1], P Adriaensens[4], G Brook[5], R Franzen[1], J Gelan[4], J Schoenen[1] and D Martin[2]

[1]Department of Neuroanatomy, Centre for Cellular and Molecular Neurobiology, University of Liège, Liège, Belgium; [2]Department of Neurosurgery, Centre Hospitalier Universitaire, Liège, Belgium; [3]Lab of Morphology, Biomedical Research Institute (BIOMED), Hasselt University, Diepenbeek, Belgium; [4]Chemistry Division, Institute for Materials Research (IMO), Hasselt University, Diepenbeek, Belgium and [5]Department of Neuropathology, Aachen University Medical School, Aachen, Germany

Study design: This was an experimental study.
Objectives: White matter sparing influences locomotor recovery after traumatic spinal cord injury (SCI). The objective of the present post-mortem magnetic resonance imaging (MRI) investigation was to assess the potential of a simple inversion recovery (IR) sequence in combination with high-resolution proton density (PD) images to selectively depict spared white matter after experimental SCI in the rat.
Setting: This study was conducted at University of Liège and Centre Hospitalier Universitaire, Liège, Belgium and Hasselt University, Diepenbeek, Belgium.
Methods: Post-mortem 9.4 tesla (T) MRI was obtained from five excised rat spines 2 months after compressive SCI. The locomotor recovery had been followed weekly using the standardized Basso–Beattie–Bresnahan scale. IR MRI was used to depict normal white matter as very hypo-intense. Preserved white matter, cord atrophy and lesion volume were assessed, and histology was used to confirm MRI data.
Results: MRI showed lesion severity and white matter sparing in accordance with the degree of locomotor recovery. IR MRI enhanced detection of spared and injured white matter by selectively altering the signal of spared white matter. Even subtle white matter changes could be detected, increasing diagnostic accuracy as compared to PD alone. MRI accuracy was confirmed by histology.
Conclusion: High-resolution IR-supported PD MRI provides useful micro-anatomical information about white matter damage and sparing in the post-mortem assessment of chronic rat SCI.
Spinal Cord (2011) **49,** 345–351; doi:10.1038/sc.2010.129; published online 28 September 2010

Keywords: spinal cord injury; rat; magnetic resonance imaging; proton density; inversion recovery; white matter sparing

Introduction

After incomplete spinal cord injury (SCI), the most common type of human traumatic SCI,[1] some white matter is spared. After experimental SCI, white matter preservation has been shown to influence the functional re-organization of the sublesional spinal cord, locomotor function and recovery.[2] Since the 1990s, correlations between magnetic resonance imaging (MRI), histology and behavioural recovery[3] have been established, initially using low-resolution images for approximate qualitative assessments of lesion extent and parenchymal sparing.[4,5] For example, experimental *in vivo* 4.7 T MRI 3 months after incomplete SCI in the rat established weak correlations between recovery and MRI-measured lesion surface and lesion volume; the post-mortem histological analysis showed a correlation of recovery with the degree of white matter sparing.[6] The amount of spared white matter thus appears as the key factor in locomotor recovery.

With the evolution of MRI technology, it is possible to obtain very high resolution MR images. We recently described rapid and precise post-mortem 9.4 T spinal cord-spine block proton density (PD)-weighted MRI after experimental rat SCI.[7]

Inversion recovery (IR) imaging provides the capacity to remove the MR signal of a specifically selected biological

Correspondence: Dr F Scholtes, Department of Neuroanatomy, Centre for Cellular and Molecular Neurobiology, University of Liège, Sart Tilman Bat. B35, Liège 4000, Belgium.
E-mail: Felix.Scholtes@chu.ulg.ac.be
Received 11 September 2009; revised 25 May 2010; accepted 5 August 2010; published online 28 September 2010

tissue from MR images, because water molecules have a unique T1 relaxation behaviour depending on their environment, that is, tissue structure. This relaxation behaviour is characterized by a specific T1 relaxation decay time. The removal of the signal from a selected tissue by IR results in a very hypo-intense signal intensity for the corresponding tissue in the image.

In this investigation, we thus address the usefulness of IR-supported PD MRI for the selective assessment of white matter sparing after incomplete SCI in the rat.

Materials and methods

Surgery

A partial low thoracic SCI was created in five rats using subdural balloon inflation as described in detail before[8] with 20 μl sterile saline for 5 min at the tenth thoracic level. After removal of the balloon, muscles and skin were closed in two layers. Balloon dysfunction (unexpected abnormal inflation shape) was detected during surgery. Therefore, in this series of rats, the traumatic lesions of the cord were variable, due to the irregular inflation of the balloon.

Immediately after surgery, dehydration was prevented by intraperitoneal physiological saline injections and infection by intraperitoneal injection of amoxicillin–clavulanic acid. The bladder was manually expressed daily until recovery of spontaneous micturition. Urinary infections were treated as needed. Rats were housed separately. Food and water were provided *ad libitum*.

Behavioural analysis

Motor function of the hind limbs was evaluated weekly using the Basso–Beattie–Bresnahan (BBB) open-field locomotor test, from 4 days postoperatively (week 1) until the week.[8] Before observation, bladders were emptied to avoid hind limb activity associated with voiding. Two examiners scored locomotion in a blinded manner from 0 to 21 for both hind limbs over 5 min in a standardized open field.

MRI

After 9 weeks, the animals were deeply anaesthetized with 1.5 mg kg^{-1} pentobarbital and perfused with 4% paraformaldehyde in 1.0 M phosphate. The spine was removed and post-fixated in 4% paraformaldehyde for 48 h, then stored for MRI in phosphate-buffered saline/azide.

Spine specimens, centred on the lesion, were analysed with a 25 mm diameter birdcage coil in a 9.4 T vertical bore magnet (Varian Inova 400 Spectrometer; Varian, Nuclear Magnetic Resonance Instruments, Palo Alto, CA, USA). Consecutive 1 mm slices were obtained in an axial slice direction using the multi-slice spin-warp technique. PD images were acquired over a length of 23 mm with a repetition time (TR) and an echo time (TE) of 2500 and 18 ms, respectively. High-resolution PD images (in-plane resolution of 37.8 μm × 37.8 μm, FOV = 17 mm × 17 mm, data matrix = 450 × 450) were acquired with a number of averages (NA) of 32 in a total acquisition time (tat) of about 10 h. Medium-resolution PD images (68 μm × 68 μm, FOV = 17 mm × 17 mm, data matrix = 250 × 250) were acquired with NA = 4 (tat of 40 min).

We used an IR time (TI) of 525 ms to selectively suppress the signal of normal, spared white matter, optimized for formaline fixed spinal cord tissue at 9.4 T. Medium-resolution IR images (68 μm × 68 μm, TR = 2500 ms, TE = 18 ms, TI = 525 ms and NA = 16) were acquired over a distance of 11 mm centred on the lesion (tat of 7 h). Preliminary IR images were obtained at a resolution of 100 μm × 100 μm and NA = 4 (tat of 1 h 20 min) but not systematically used for the present study.

The tomographic right side corresponded to the anatomical left side, and *vice versa*.

Histology

After removal from the spine and cryoprotection for 48 h in 30% sucrose at 4 °C, the spinal cords were cut axially at a thickness of 15 μm on a cryostat, mounted onto gelatine-coated slides and stained with Luxol Fast Blue for myelin and haematoxylin.

Morphometry

Data for morphometry were obtained using the Olympus Analysis FIVE software (Olympus Europa GmbH, Hamburg, Germany) for manual delineation of surfaces and automatic calculation of the surface area. When there were several lesion areas, surface measurements were added. Areas were expressed in μm^2 and volumes in μl. For MR images, the measured area was multiplied with the pixel dimensions. Two observers, who were blinded to BBB scores, determined lesion versus spared tissue, then delineated the axial lesion extent on digitalized histological and MR images. MR and histological images were assessed independently. For MRI measurements, PD and IR images were used simultaneously to define very hypo-intense IR signal as spared white matter when this hypo-intensity was not observed in the PD image. Hypo-intensity present in IR as well as in PD images was considered to be due to the presence of iron, that is, secondary to haemorrhage. Morphometry was then performed on the PD images. For histological measurements, 1 out of 33 sections was analysed in the periphery of the lesion centre (two 6 mm blocks) and 1 out of 22 in the central block (11 mm), resulting in 10 peripheral sections and 30 central sections. Measurements were only performed on sections that showed a lesion. Low- and high-resolution microscopy was used to interpret the images and distinguish the lesion from spared tissue.

In addition to spared white matter, measured surface areas were total spinal cord area and lesion area. Atrophy of the spinal cord was defined as the minimal total cord surface measured in each cord. Lesion volume was calculated as the area under the curve of the lesion surface measurements; missing histological data points (due to non-interpretability of some histological slices) were compensated for by inserting the mean of the two adjacent values.

On the basis of the different measurements, we established graphs, showing the MRI section number on the *x* axis and

the surface measurements on the *y* axis in μm^2, depicting cord atrophy, lesion size and spared matter (Figure 1). Non-quantitative correlative figures were created to visually correlate MRI and histological measurements.

Ethics statement

We certify that all applicable institutional and governmental regulations concerning the ethical use of animals were followed during the course of this research.

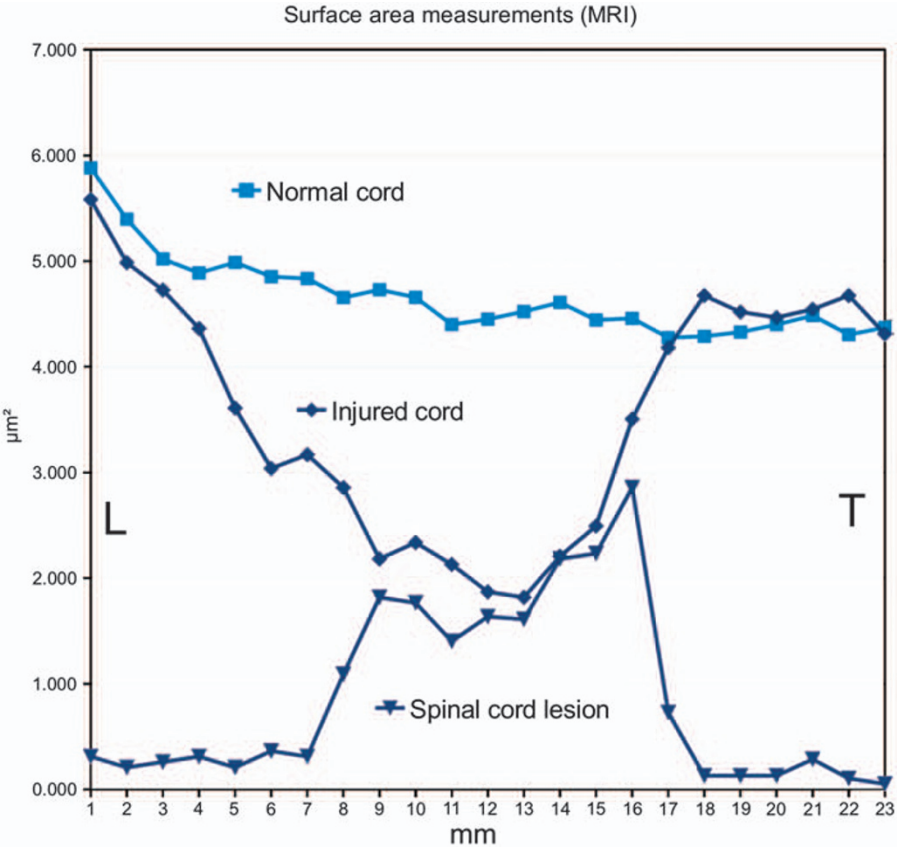

Figure 1 Plotting of MRI surface measurements from the lumbar (L) to the thoracic (T) level. The upper light blue curve shows the surface area measurements of transverse MRI sections of an uninjured cord. The upper dark blue curve corresponds to the surface measurements of the total surface of the injured cord, and the lower curve to the surface measurement of the lesion.

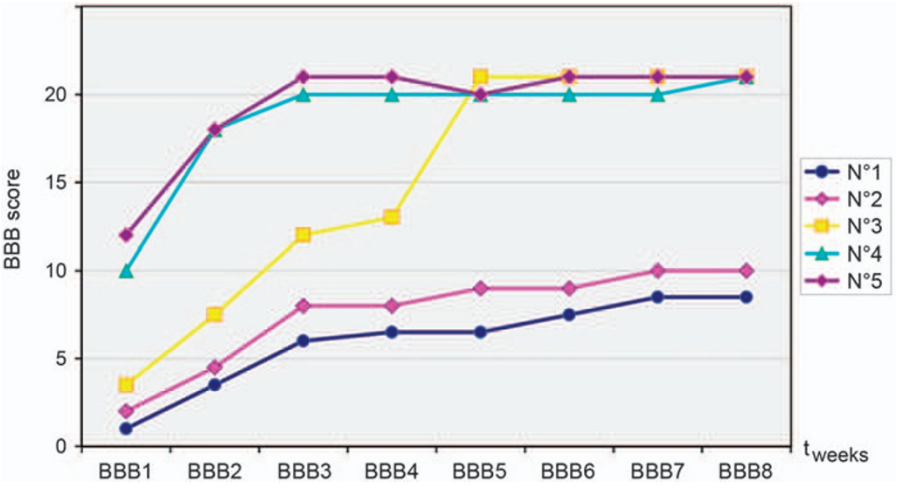

Figure 2 BBB evolution. Rats 1 and 2 showed limited recovery. Final BBB scores were 8.5 for rat 1, corresponding to plantar placement of the paw on one side and plantar placement with weight support on the other, and 10 for rat 2, corresponding to occasional stepping movements without forelimb–hindlimb coordination. Rat 3 showed slow recovery up to the maximal score of 21. Rats 4 and 5 showed rapid recovery of practically normal over-ground locomotion.

Results

Locomotor recovery

Three recovery patterns could be distinguished (Figure 2). Rats 1 and 2 showed limited recovery, rat 3 slow recovery up to the maximal score of 21, and rats 4 and 5 rapid and complete recovery of practically normal over-ground locomotion.

MRI and histology

As confirmed by histology, gliotic scarring appeared hyper-intense on PD-weighted images. Haemorrhage was responsible for low signal intensity because of hemosiderin-containing ferric iron. IR images increased the contrast between white matter (very hypo-intense) and gliosis, and even very discrete white matter changes, almost imperceptible and difficult to interpret on PD images, could be ascertained (Figure 3). The topographical correlation between MRI and histology was precise: white matter preservation, spinal cord shape and lesion extent were congruent (Figure 4). When the interpretation of the presence of preserved white matter was based on the combined analysis of the PD and the IR images, histology confirmed the result in every case. Vacuolation of the white matter appears clearly on the IR images, but not so on the standard PD-weighted images. Cord atrophy was severe. Some cords show the presence of a liquid-filled cyst. Extensive gliosis (hyper-intense) with evidence for haemorrhage (hypo-intense) was observed at the centre of lesion.

Morphometry quantified the differences in atropy, lesion size and white matter sparing (Table 1), as expected from the locomotor behaviour of the three animals. On the non-quantitative comparative graphs (Figure 5), the pattern of lesion distribution and extent, from the lumbar to the thoracic region, MRI was congruent with histology. The ratio of histological to MRI measurements was variable, though in most cases approximately 0.5 (range 0.42–0.81). The assessment of lesion severity and parenchymal sparing was in accordance with the BBB evolution.

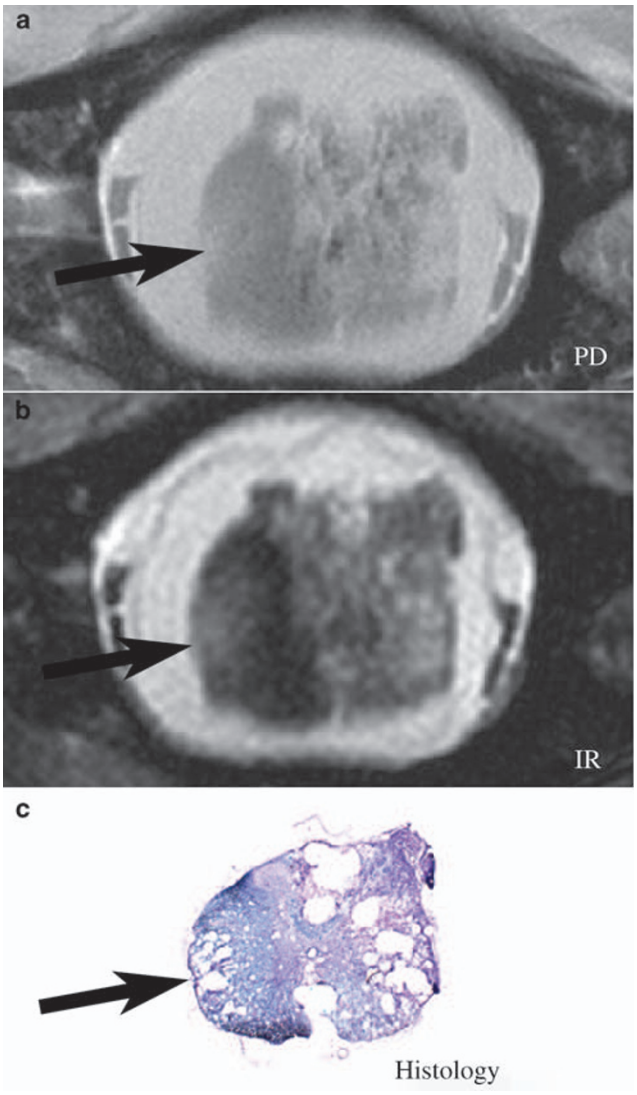

Figure 3 White matter damage demonstrated by PD (**a**) and IR (**b**) MRI, confirmed by histology (**c**, haematoxylin–Luxol Fast Blue). Severe damage is detected by both imaging techniques, although contrast is higher in IR images (anatomical left side half of the cord, on the right of the cord image). More subtle white matter changes that cannot unequivocally be shown on standard PD-weighted images appear clearly on the IR images. The latter showed a white matter lesion (arrows) in the right lateral funiculus with superior contrast to the standard PD image. Rat 4.

Discussion

This investigation shows that IR MRI can be a simple and efficient complement to fast, medium-resolution PD MRI for visualizing white matter after experimental compressive SCI. Histology confirmed that IR enhanced the detection of white matter abnormalities. This technique reveals even discrete changes, such as vacuolation in the descending white matter tracts. The functional significance of these discrete changes is not clearly established. However, their detection by IR MRI shows its diagnostic precision for a key factor in locomotor recovery after SCI: white matter damage versus sparing.[2]

Inversion recovery MRI of the completely excised, fixated spine is performed before tissue manipulations and freezing, unlike histology.[7] MRI thus localizes abnormal signal and spared matter with micro-anatomical certainty, because of the absence of cord deformation. This localization is important because the descending tracts involved in locomotor recovery follow a precise distribution mainly in the anterior and lateral funiculi.[9,10]

In addition, MRI-based measurements of lesion size, cord atrophy and spared matter may be more accurate than histological microscopy, despite the lower resolution of MRI, because of the absence of tissue deformation. This is underlined in this investigation by the observed variable ratios of histological to MRI measurements, indicating that the spinal cord undergoes changes during the preparation for histology, including retraction during the freezing process.

The spatial precision (that is, MR image resolution) of the present technique appears useful for future correlation of MRI with locomotor recovery. Although anatomically

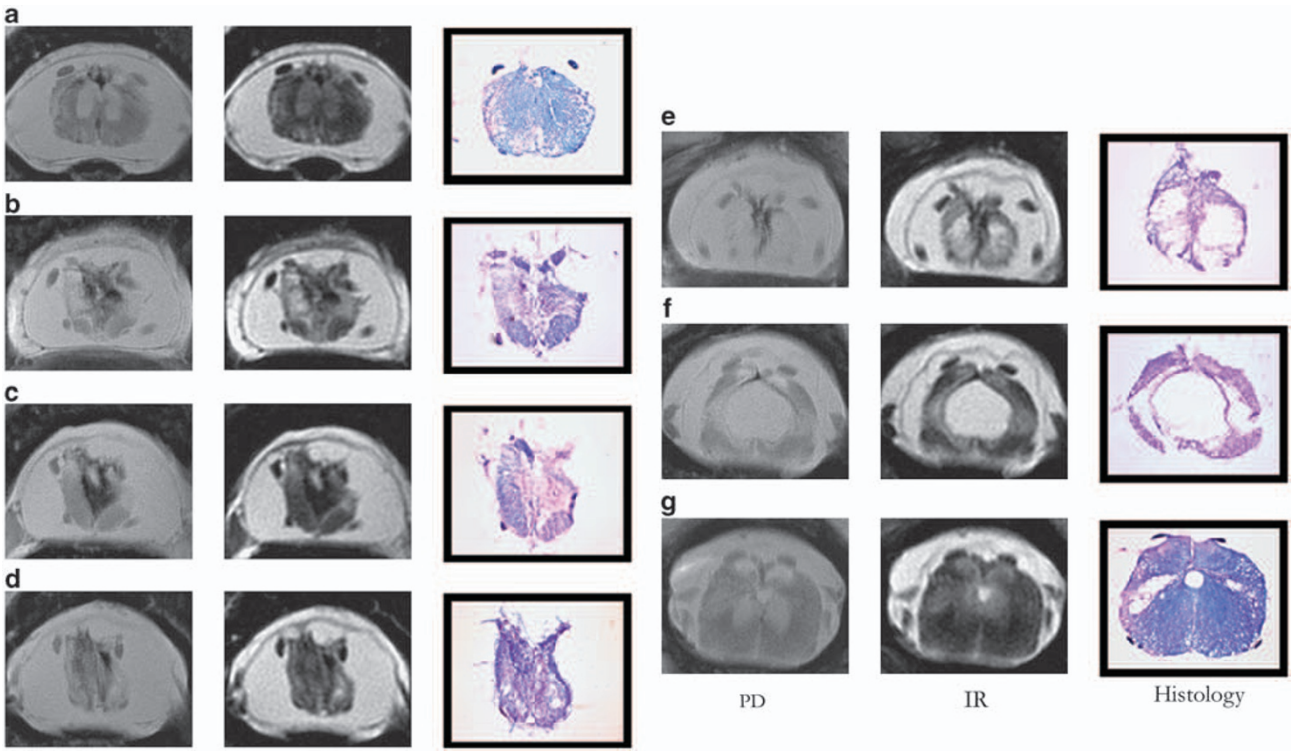

Figure 4 Correlation of PD and IR MRI with histology (rat 1). Proton density-weighted MRI (left column, resolution 37.8 μm × 37.8 μm per pixel), inversion recovery (middle column, resolution 68 μm × 68 μm per pixel) and histology (right column), from caudal (**a**) to rostral (**g**). This sequence illustrates the usefulness of inversion-recovery imaging for the detection of white matter damage over the length of the spinal cord lesion. (**a**) Lumbar extremity of the lesion zone with beginning cord atrophy. The main lesion is seen in the posterior cord, between the dorsal horns. Some white matter vacuolation can be seen in the periphery. (**b**) The topography of hemosiderin deposits in the centre of the cord (hypo-intense) and of bilateral ventral white matter sparing are matched between MRI and histology. (**c**, **e**) The progressive atrophic deformation of the cord and the lesion topography are congruent between histology and MRI. (**f**) Cystic degeneration of the lesion in the centre of the cord, surrounded by preserved white matter in the lateral funiculi. (**g**) Proximal lesion periphery with ventral vacuolation of white matter. Central atrophic scarring resulting in the juxtaposition of the hyper-intense dorsal horns and a wing-shaped extension of the lesion into the lateral cord.

Table 1 Morphometric data

	Rat 1	*Rat 2*	*Rat 3*	*Rat 4*	*Rat 5*
Lesion volume (μl)	22.33	22.39	15.45	10.74	5.13
Atrophy (minimal cord surface: mm^2)	2.45	1.88	3.56	3.90	5.46
Minimal spared white matter* (mm^2)	0.13	0.32	0.96	1.30	2.39

Morphometric data derived from PD-weighted MRI with support of IR images.
*Minimal white matter sparing was the amount of spared matter assessed in the single MRI section where this white matter surface area was minimal.

confined, the nerve fibres controlling basic locomotion are diffuse, rather than forming precisely limited, small tracts,[9–11] and assessment with the presently shown resolution is sufficient to estimate damage to these large tracts. In this investigation, the behavioural data were in gross accordance with the lesion severity and white matter sparing. Even, the combination of rapidly acquired PD-weighted images with 'low-resolution' IR images (for example, 100 μm per pixel, which can be obtained in less than 1 h 1/2 with NA = 4) may provide sufficiently high diagnostic accuracy, and this should be systematically investigated in the future.

The present MRI settings cannot be used *in vivo* due to the long acquisition time, the limited axial size of the rat spinal cord and other technical constraints. However, they can be used on human post-mortem material, including PD imaging.[12] In the long run, the transfer of this kind of sequence to *in vivo* high-resolution rat[13,14] or even mouse[15] spinal cord MRI may be feasible if faster image acquisition proves to be of sufficient quality. With *in vivo* MRI, the present assessment at a single time point after the recovery period (which is a significant limitation to any post-mortem investigation) could be overcome and replaced by a continuous assessment of the lesion and correlation with behavioural parameters.

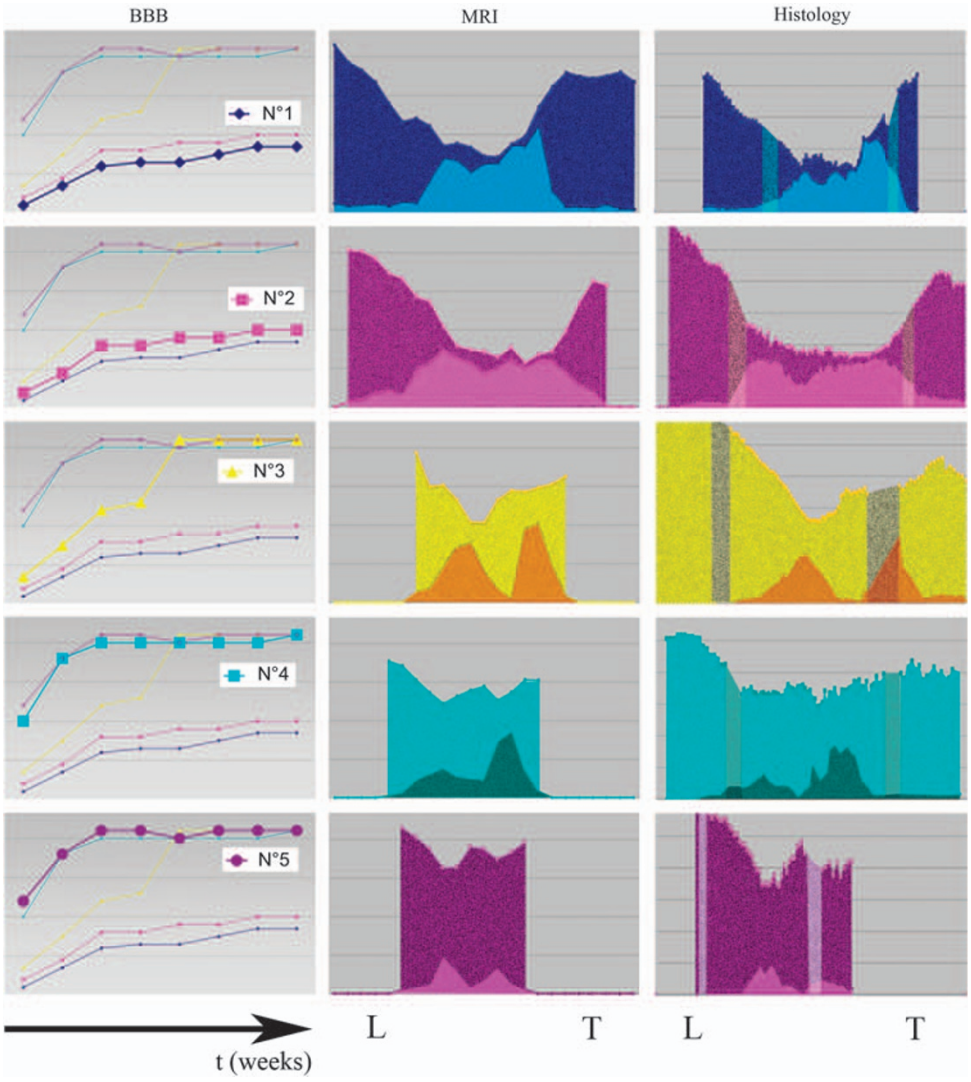

Figure 5 Illustrative graph correlating BBB evolution curves (left column), spared matter, atrophy and lesion severity measured on the MR images (PD, middle column) and histology (right column). The upper curves correspond to the cord surface measurements and the lower curves to the lesion surface measurements. The graphs have been created with the same scale for each rat (see Figure 1), but the scales have been omitted in this figure for clarity. In the histological measurements, tissue loss at the end of the section blocks had resulted in missing surface measurements, which are accounted for by the differently shaded surfaces.

Conclusion

This investigation shows the precision of the micro-anatomical spinal cord white matter assessment using post-mortem IR-supported PD MRI of the injured rat spinal cord within the spine. The combined technique is efficient in terms of acquisition speed, contrast, signal-to-noise ratio and resolution. Images with a high diagnostic yield can be acquired within short time periods.

Conflict of interest

The authors declare no conflict of interest.

Acknowledgements

This research was sponsored by grants from the Fond National de la Recherche Scientifique (FNRS, Belgium)/Fonds voor Wetenschappelijk Onderzoek grant (FWO, Belgium) and supported by the Belgian Society of Neurosurgery (Bayer-Schering-Pharma grant, Felix Scholtes). At the time most of the experiments were carried out, Felix Scholtes was a research fellow at the FNRS, Belgium. We acknowledge the financial support from tUL impuls financiering.

References

1 Miyanji F, Furlan JC, Aarabi B, Arnold PM, Fehlings MG. Acute cervical traumatic spinal cord injury: MR imaging findings correlated with neurologic outcome—prospective study with 100 consecutive patients. *Radiology* 2007; **243**: 820.
2 Basso DM. Neuroanatomical substrates of functional recovery after experimental spinal cord injury: implications of basic science research for human spinal cord injury. *Phys Ther* 2000; **80**: 808.
3 Duncan EG, Lemaire C, Armstrong RL, Tator CH, Potts DG, Linden RD. High-resolution magnetic resonance imaging of

experimental spinal cord injury in the rat. *Neurosurgery* 1992; **31**: 510.
4 Hackney DB, Ford JC, Markowitz RS, Hand CM, Joseph PM, Black P. Experimental spinal cord injury: MR correlation to intensity of injury. *J Comput Assist Tomogr* 1994; **18**: 357.
5 Hackney DB, Finkelstein SD, Hand CM, Markowitz RS, Black P. Postmortem magnetic resonance imaging of experimental spinal cord injury: magnetic resonance findings versus *in vivo* functional deficit. *Neurosurgery* 1994; **35**: 1104.
6 Metz GA, Curt A, van de Meent H, Klusman I, Schwab ME, Dietz V. Validation of the weight-drop contusion model in rats: a comparative study of human spinal cord injury. *J Neurotrauma* 2000; **17**: 1–17.
7 Scholtes F, Phan-Ba R, Theunissen E, Adriaensens P, Brook G, Franzen R *et al*. Rapid, postmortem 9.4T MRI of spinal cord injury: correlation with histology and survival times. *J Neurosci Methods* 2008; **174**: 157–167.
8 Martin D, Schoenen J, Delrée P, Gilson V, Rogister B, Leprince P *et al*. Experimental acute traumatic injury of the adult rat spinal cord by a subdural inflatable balloon: methodology, behavioral analysis, and histopathology. *J Neurosci Res* 1992; **32**: 539–550.
9 Loy DN, Magnuson DS, Zhang YP, Onifer SM, Mills MD, Cao QL *et al*. Functional redundancy of ventral spinal locomotor pathways. *J Neurosci* 2002; **22**: 315–323.
10 Schucht P, Raineteau O, Schwab ME, Fouad K. Anatomical correlates of locomotor recovery following dorsal and ventral lesions of the rat spinal cord. *Exp Neurol* 2002; **176**: 143–153.
11 Loy DN, Talbott JF, Onifer SM, Mills MD, Burke DA, Dennison JB *et al*. Both dorsal and ventral spinal cord pathways contribute to overground locomotion in the adult rat. *Exp Neurol* 2002; **177**: 575–580.
12 Scholtes F, Adriaensens P, Storme L, Buss A, Kakulas BA, Gelan J *et al*. Correlation of postmortem 9.4 tesla magnetic resonance imaging and immunohistopathology of the human thoracic spinal cord 7 months after traumatic cervical spine injury. *Neurosurgery* 59, 671–678, discussion 2006, 671-8.
13 Behr VC, Weber T, Neuberger T, Vroemen M, Weidner N, Bogdahn U *et al*. High-resolution MR imaging of the rat spinal cord *in vivo* in a wide-bore magnet at 17.6 Tesla. *MAGMA* 2004; **17**: 353–358.
14 Weber T, Vroemen M, Behr V, Neuberger T, Jakob P, Haase A *et al*. *In vivo* high-resolution MR imaging of neuropathologic changes in the injured rat spinal cord. *AJNR Am J Neuroradiol* 2006; **27**: 598–604.
15 Bilgen M, Al-Hafez B, Alrefae T, He YY, Smirnova IV, Aldur MM *et al*. Longitudinal magnetic resonance imaging of spinal cord injury in mouse: changes in signal patterns associated with the inflammatory response. *Magn Reson Imaging* 2007; **25**: 657–664.